

## Research Progress of Self-Supported Ceramic Electrodes for Water Electrolysis

Chenqi Jiang, Bo Huang, Zhijie Gao, Hengfeng Sheng, Weifeng Du, Xingqun Zhu\*

School of Materials Science and Engineering, Xuzhou University of Technology, Xuzhou  
221018, China

\*Corresponding Author

### Abstract

As global demand for sustainable energy grows, hydrogen has emerged as a clean and efficient energy carrier, attracting widespread attention. Water electrolysis, an environmentally friendly hydrogen production method, generates only hydrogen and oxygen without greenhouse gas emissions. In this process, catalysts play a pivotal role. Conventional powdered catalysts often suffer from low conductivity, inefficient hydrogen evolution, and poor recoverability. While loading catalysts onto substrates such as nickel foam or carbon materials can enhance conductivity, these supports typically exhibit low mechanical strength, poor resistance to strong acids or alkalis, and limited adaptability. In contrast, emerging ceramic membrane electrodes offer significant advantages, including high stability, durability, and resistance to physical damage. These properties make them promising candidates for water electrolysis applications. This short review summarizes recent advances in the preparation of ceramic membrane electrodes and their performance in water electrolysis.

### Keywords

Self-supported Ceramic Electrodes (SSCEs); Water Electrolysis; Hydrogen Production; Electrocatalysis; Porous Structure Design; Heterojunction Engineering.

### 1. Introduction

The extensive reliance on fossil fuels has dramatically increased atmospheric CO<sub>2</sub> concentrations, accelerating global warming at an unprecedented rate. Decades of unsustainable fossil fuel consumption have not only caused severe environmental degradation but also contributed to the current global energy crisis. Hydrogen energy, as a clean secondary energy carrier, plays a pivotal role in achieving carbon neutrality goals worldwide. Unlike fossil fuels, hydrogen combustion produces only water vapor, eliminating carbon emissions and other harmful pollutants entirely. This unique characteristic positions hydrogen as a key driver for deep decarbonization across various sectors, such as transportation, industry, and power generation [1,2]. Furthermore, hydrogen's exceptional energy storage capacity facilitates the effective integration of intermittent renewable energy sources such as wind and solar power, thereby accelerating the transition toward diversified, low-carbon energy systems.

Water electrolysis is a cornerstone technology for green hydrogen production, utilizing electrical energy to split water into hydrogen and oxygen [3]. When powered by renewable energy sources (e.g., wind, solar), it enables carbon-free hydrogen production, ensuring sustainability from the outset. Moreover, water electrolysis systems exhibit high operational flexibility, allowing rapid response to grid fluctuations-enhancing renewable energy integration while contributing to grid stability. As a critical nexus between power systems and the hydrogen value chain, electrolysis plays a pivotal role in establishing an integrated "electricity-hydrogen-utilization" system, advancing a cleaner and more resilient energy future.

Conventional powder catalysts suffer from inherent limitations, including poor conductivity, low hydrogen evolution efficiency, and challenging recovery processes. Although supported catalysts (e.g., those using nickel foam or carbon substrates) improve electrical conductivity, they often exhibit low mechanical strength, poor resistance to strong acids/alkalis, and limited operational adaptability. In contrast, noble metal-based electrodes demonstrate superior HER and OER performance [4,5]. Nevertheless, their high price and the shortage of earth resources suppress their potential for large-scale application. Self-supported ceramic electrodes (SSCEs) have emerged as a highly promising alternative, combining binder-free integrated structures, exceptional mechanical strength (e.g., TiN ceramics with a bending strength of 36.6 MPa) [6,7], and engineered porous architectures that enhance mass transport and gas release. Unlike powder-based electrodes, SSCEs directly grow the catalyst on a conductive substrate, eliminating the need for binders and their associated drawbacks [8]. This design not only enhances electrocatalytic activity and stability but also prevents active site blockage and conductivity reduction caused by polymer binders [9-12].

This review comprehensively summarizes the design strategies, fabrication techniques, and performance optimization of SSCEs, while analyzing current challenges and future directions to advance their industrial application in water electrolysis.

## 2. Classification and Design Strategies of SSCEs

### 2.1. Material Types

The superior performance of SSCEs stems from rational material selection and structural engineering, which synergistically enhance conductivity, catalytic activity, and durability.

#### 2.1.1. Conductive Ceramics

Conductive ceramics are ideal electrode substrates owing to their exceptional combination of high electrical conductivity and superior chemical stability. Among them, transition metal carbides (TMCs), including WC [13], Mo<sub>2</sub>C [14], and Ni<sub>3</sub>C [15], have emerged as promising noble-metal-free electrocatalysts due to their earth-abundant nature and outstanding electrical properties. For example, titanium carbide (TiC) demonstrates remarkable electrical conductivity (10<sup>5</sup>–10<sup>6</sup> S/m) and an ultra-high melting point (3067°C), enabling stable performance even in highly corrosive acidic or alkaline environments. These properties make TiC an excellent catalyst support, as demonstrated in TiC@MoS<sub>2</sub> composite electrodes [16]. Similarly, titanium nitride (TiN) retains its porous structure even after high-temperature sintering at 1600°C, exhibiting low resistivity (0.23 mΩ·cm<sup>-1</sup>) and high mechanical strength (36.6 MPa in bending) [17]. TiC<sub>0.5</sub>N<sub>0.5</sub> ceramic membrane combines the advantages of TiC and TiN ceramics [16-18]. Tungsten carbide (WC), which exhibits a platinum-like electronic structure, can achieve significantly enhanced catalytic activity through nitrogen doping (forming WC-N/W heterojunctions) or oxygen vacancy engineering (yielding WC/WO<sub>3-x</sub> heterojunctions) [13]. For instance, the WC-N/W electrode demonstrates an exceptionally low hydrogen evolution overpotential of 87 mV in acidic media. Regarding catalyst supports, tantalum carbide (TaC) stands out as an ultra-high-temperature ceramic, boasting an exceptionally high melting point (3880°C), hardness (20 GPa), and elastic modulus (450 GPa), along with excellent electrical and thermal conductivity [19,20]. Another notable molybdenum-based structural ceramic, MoSi<sub>2</sub> [21], has found widespread application in electric heating elements and has attracted significant attention in electrocatalysis research due to its high electrical/thermal conductivity, outstanding mechanical properties, and superior high-temperature oxidation resistance [22].

### 2.1.2. Composite Ceramics

Composite ceramics achieve synergistic performance enhancement through heterostructure engineering. Previous studies have demonstrated that molybdenum-based catalysts, including MoS<sub>2</sub> [23,24], Mo<sub>2</sub>C [25,26], Mo<sub>2</sub>N [27,28], and MoB<sub>2</sub> [29], exhibit excellent water electrolysis activity. For example, TiC@MoS<sub>2</sub> enhances electron transfer efficiency via lattice matching between TiC and 1T-2H phase MoS<sub>2</sub>, with the 1T-MoS<sub>2</sub>/TiC interface exhibiting an optimal hydrogen adsorption free energy ( $\Delta G_H$ )\* of 0.116 eV. Similarly, MoO<sub>2</sub> has been widely employed as an electrochemical water-splitting catalyst due to its high electrical conductivity, outstanding chemical stability, and efficient charge transport capabilities [28-31]. The Co<sub>0.9</sub>Ni<sub>0.1</sub>P/TiC<sub>0.5</sub>N<sub>0.5</sub> system further optimizes hydrogen adsorption energy through strong electronic interactions between bimetallic phosphides and the titanium carbonitride substrate, achieving an exceptionally low  $\Delta G_H$  of -0.039 eV\*. Other composite systems, such as MoO<sub>2</sub>/MoSi<sub>2</sub> and Ni@TiC, effectively balance electrical conductivity and catalytic activity via multi-phase synergistic effects.

**Table 1.** Performance Comparison Table of Conductive Ceramics and Composite Ceramics

Material Category	Representative Materials	Electrical Conductivity	Mechanical Strength	Typical Advantages	Application Scenarios	Ref.
Conductive Ceramics	TiC, TiN, WC	10 <sup>5</sup> -10 <sup>6</sup> S/m (TiC)	36.6 MPa (TiN, bending)	High chemical stability, corrosion resistance	Acid/alkaline electrolytes	[32]
Composite Ceramics	TiC@MoS <sub>2</sub> , Co <sub>0.9</sub> Ni <sub>0.1</sub> P/TiC <sub>0.5</sub> N <sub>0.5</sub>	Dependent on components	Enhanced by heterostructure	Synergistic activity, optimized $\Delta G_H$ *	Bifunctional HER/OER in alkaline media	[33]

## 2.2. Structural Design

The structural design of electrode materials plays a pivotal role in regulating their electrochemical performance. By precisely tailoring pore characteristics and spatial configurations, it is possible to achieve a synergistic optimization of specific surface area, mass transfer efficiency, and mechanical stability. This optimization provides a critical foundation for the efficient application of electrodes in energy conversion and storage systems.

### 2.2.1. Porous Architectures

Porous conductive ceramics represent attractive self-supported electrode materials due to their exceptional thermal/chemical stability, tunable pore structures, and high mechanical strength[34]. Porous architectures, as one of the most prevalent structural designs, can construct asymmetric structures encompassing skin layers, finger-like pore layers, and sponge layers via phase inversion tape casting. The key advantage of this layered design lies in its multifunctional architecture: the dense skin layer effectively minimizes electrolyte leakage while improving structural integrity, the interconnected finger-like pore layer facilitates rapid mass transport, and the sponge layer substantially enhances the specific surface area due to its abundant microporous structure. Moreover, this multi-layer architecture enables a more rational stress distribution during operation, significantly mitigating the risk of structural damage [35]. For instance, the TiN ceramic electrode fabricated using this method (Figure 1) exhibits well-defined straight pores with diameters of 50–60  $\mu\text{m}$  and a high porosity of 62.5% [36]. This unique structure endows the electrode with a remarkable double-layer capacitance of 504 mF/cm<sup>2</sup>-far exceeding that of conventional dense structural materials. Furthermore, a gradient pore design can further enhance mass transfer efficiency while maintaining

mechanical strength. By tailoring the pore distribution from the surface to the substrate (e.g., combining a dense SiOC coating with a porous ceramic matrix) [37], this approach aligns with the growing trend toward multifunctional material integration. A notable example is the  $\text{MoO}_2/\text{MoSi}_2$  composite ceramic, whose gradient pore architecture yields a high specific surface area of  $14.286 \text{ m}^2 \cdot \text{g}^{-1}$ , demonstrating exceptional activity and stability in electrocatalytic reactions [29]. Nitrogen adsorption-desorption analysis revealed a type II isotherm with a hysteresis loop, confirming the mesoporous characteristics of the material.

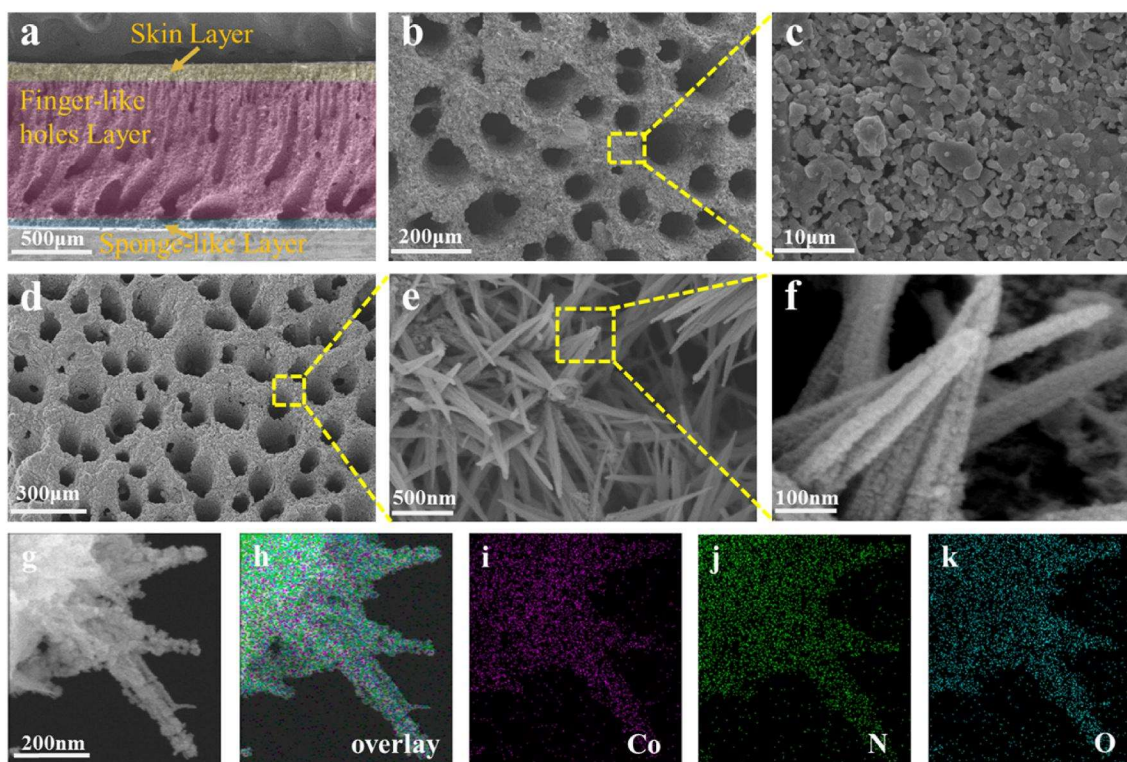


**Figure 1.** Microstructure of TiN ceramic membrane and NCTN-350-2. (a) Cross-section shows layered structure with finger-like holes (directional straight pores for gas-liquid transport, as discussed). (b-f) SEM images of NCTN-350-2. (g-k) STEM & EDS mapping of NCTN-350-2 [36].

### 2.2.2. Directional Straight Pores

Directional straight pores exhibit exceptional performance in facilitating gas-liquid transport and bubble release due to their vertically aligned channel architecture. These structures are typically fabricated using directional freeze-drying technology, which involves controlling the growth direction of ice crystals to form aligned pore channels that remain interconnected after degreasing and sintering [29]. A representative example is the  $\text{MoO}_2/\text{Mo}_2\text{C}$  electrode prepared by this method, which features pore diameters of approximately  $100 \mu\text{m}$  [29]. The directional pore channels reduce hydrogen diffusion resistance by over 40%, effectively mitigating the issue of active site blockage caused by bubble accumulation in conventional porous materials. For tungsten carbide (WC)-based electrodes, the benefits of directional straight pores are even more pronounced. Even at high current densities ( $30\text{--}1000 \text{ mA} \cdot \text{cm}^{-2}$ ), the aligned channels enable rapid gas expulsion, ensuring long-term electrode stability and providing robust structural support for high-current-density electrolytic hydrogen production [29].

### 2.2.3. 3D Self-Supporting Configurations

3D self-supporting electrode architectures fundamentally overcome the limitations of conventional electrodes by eliminating binder-induced active site blockage and minimizing interfacial resistance through integrated binder-free and substrate-free design [29,38]. These

structures are typically fabricated via template-assisted or in-situ growth methods. A representative example is the Co/CoSe membrane [32], which features an ~800  $\mu\text{m}$  thick structure composed of interconnected conductive skeletons and finger-like pore networks. The robust skeletons provide excellent electrical conductivity and mechanical stability, while the hierarchical pore structure enables efficient electrolyte penetration and rapid gas evolution. This innovative design achieves more than a 30% improvement in active material utilization while dramatically reducing charge transfer resistance by eliminating interfacial contact losses. As a result, such electrodes demonstrate superior energy conversion efficiency in electrocatalytic processes, including hydrogen and oxygen evolution reactions.

**Table 2.** Performance Comparison of Representative Self-Supported Ceramic Electrodes(SSCEs)

Material	Structure	HER Overpotential@ 10 mA/cm <sup>2</sup> (mV)	Stability (h)	Conductivity (S/m)	Ref.
TiN	Porous asymmetric	95 (acidic)	150	10 <sup>5</sup> - 10 <sup>6</sup>	[32]
WC - N/W	Directional straight pores	87 (acidic)	220	1.4×10 <sup>6</sup>	[33]
Co <sub>4-x</sub> Fe <sub>x</sub> TiC <sub>0.53x</sub> P/TiC <sub>0.5</sub> N <sub>0.5</sub>	3D self supporting	70.4 (alkaline)	200	—	[39]
Ni@TiC	Porous	60 (HER, alkaline); 138 (OER)	50,000 cycles	—	[40]
High - entropy ceramic	Gradient pores	82 (seawater)	500	8×10 <sup>4</sup>	[41]

### 3. Fabrication Techniques

#### 3.1. Traditional Method

The fabrication of self-supporting ceramic electrodes (SSCEs) involves a delicate balance between microstructural control, compositional uniformity, and scalable production. Various technical approaches, each with distinct principles and characteristics, contribute uniquely to optimizing electrode performance. Together, these methods facilitate the transition of SSCEs from laboratory-scale development to practical industrial applications.

##### 3.1.1. Sintering (Solid-state Reaction Sintering)

Traditional fabrication methods, grounded in fundamental ceramic processing, offer unique advantages in ensuring mechanical stability and scalability. Sintering (solid-state reaction sintering) facilitates atomic diffusion at elevated temperatures, effectively bonding ceramic powder particles into a cohesive structure. For instance, pressureless sintering of MoSi<sub>2</sub> at 1400–1500°C in an argon atmosphere promotes particle consolidation, yielding a porous framework with a bending strength of 27.2 ± 3.5 MPa—a critical property for withstanding harsh high-temperature electrochemical environments [29]. Similarly, TiN ceramics sintered at 1600°C for 4 hours develop a dense yet porous skeleton, simultaneously ensuring mechanical integrity and facilitating electrolyte transport [33]. By integrating innovative materials and structural designs, these methods achieve an optimal balance between mechanical robustness and electrochemical performance.

##### 3.1.2. Slurry Coating-high Temperature Treatment Method

The slurry coating-high temperature treatment method enables scalable electrode production through a synergistic two-step process. First, ceramic powders (e.g., TiC or TiN) are dispersed

in NMP-based solvents to form homogeneous slurries, which are then coated onto substrates via tape casting to create thin films. Subsequent thermal curing and sintering complete the final shaping process [33]. Among these techniques, phase inversion tape casting stands out for its ability to form asymmetric pore structures (combining finger-like macrochannels and sponge-like micropores) in green bodies through water-induced phase separation. Importantly, this hierarchical porosity is preserved during sintering. This approach has enabled large-area fabrication of TiN and TiC membranes with porosities up to 62.5%, demonstrating successful industrial-scale production of redox flow battery electrodes and highlighting the commercial viability of traditional ceramic processing methods [33]. Further developments have expanded this methodology: Porous TaC ceramic membranes have been successfully fabricated by integrating phase inversion, tape casting, and pressureless sintering [42,43]. The phase inversion tape-casting technique reliably produces ceramic membranes with controlled asymmetric architectures (Figure 2) [44,45], which have been shown to significantly enhance HER (hydrogen evolution reaction) performance [46,47].

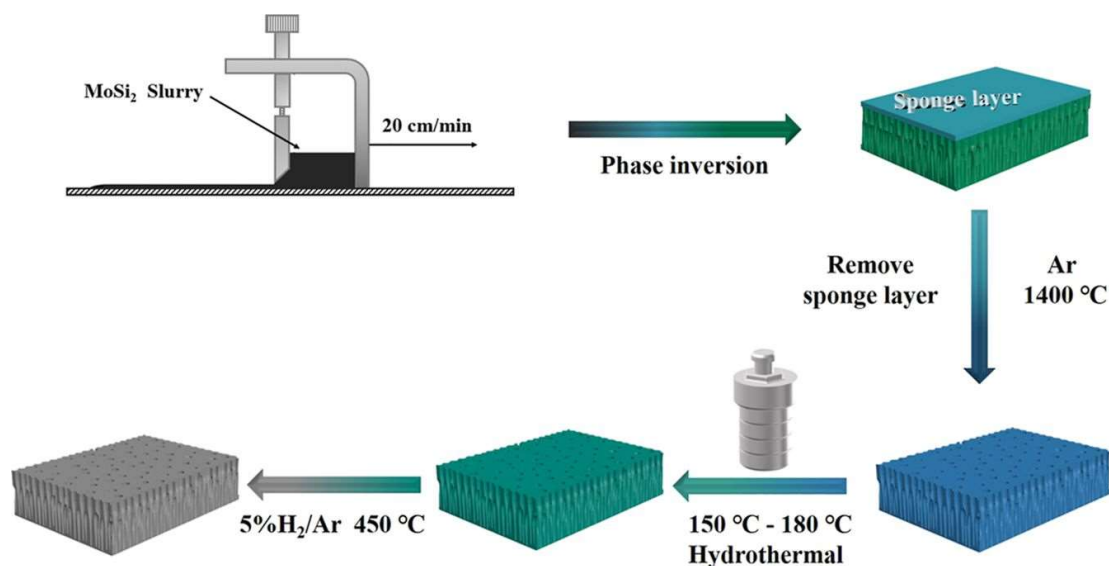


**Figure 2.** Schematic illustration of the MoO<sub>2</sub>/MoSi<sub>2</sub> ceramic electrode preparation via slurry coating [48].

## 3.2. Advanced Preparation Technology

Ongoing innovations in materials science and engineering have enabled advanced fabrication techniques to unlock new possibilities for SSCs (solid-state ceramic electrolytes), particularly through precise nanostructural and pore architecture control.

### 3.2.1. Electrospinning Technology

Electrospinning technology leverages high-voltage electric fields to transform polymer-ceramic precursor solutions into continuous nanofibers (100–500 nm in diameter), which subsequently convert into ceramic nanofiber networks upon calcination. The resulting network architecture, featuring ultrahigh specific surface areas (e.g., 150–300 m<sup>2</sup>/g for TiO<sub>2</sub>-based fibers) and percolated nanoporosity, enables rapid ion diffusion kinetics - a critical advantage for high-power applications such as supercapacitors where fast ion transport is paramount [39]. A prime example is MoO<sub>2</sub>/MoSi<sub>2</sub> nanofibers [29], fabricated through electrospinning and sintering, which demonstrate hierarchically graded porosity achieving an optimal balance between mechanical robustness (8.6 MPa tensile strength) and enhanced catalytic performance. This exemplifies the method's unique capacity for concurrent property optimization.

### 3.2.2. 3D Printing

As a prominent additive manufacturing technique, 3D printing enables unprecedented control over electrode pore architecture design [48,49]. Advanced methods like direct ink writing (DIW) and stereolithography can precisely fabricate diverse pore geometries (e.g., lattice, honeycomb) with sub-100  $\mu\text{m}$  resolution. This process involves layer-by-layer deposition of ceramic nanoparticle-based inks, which retain their designed porous structures after sintering, creating precisely engineered pathways for optimized gas-liquid transport. The precise pore gradient engineering (20–200  $\mu\text{m}$ ) in 3D-printed WC electrodes yields a 30% enhancement in mass transport kinetics compared to powder-sintered electrodes, highlighting additive manufacturing's capability for performance-driven electrode design [50].

### 3.2.3. Vapor Deposition Techniques (CVD/PVD)

Vapor deposition (CVD/PVD) provides unparalleled control over electrode surface engineering, enabling atomic-level tuning of active sites. In CVD, precursors such as  $\text{W}(\text{CO})_6$  or  $\text{TiCl}_4$  undergo gas-phase reactions to form uniform thin films (5–50 nm) on ceramic substrates [51]. Notably,  $\text{NH}_3$ -assisted CVD creates nitrogen-doped WC heterostructures (WC-N/W), which exhibit a near-ideal hydrogen adsorption free energy (0.05 eV), dramatically improving catalytic efficiency [36]. Alternatively, magnetron sputtering (PVD) applies conformal Pt/Ni layers to TiC/TiN, enhancing charge transfer without obstructing pore networks—thereby maintaining both electrochemical activity and structural stability [29].

## 3.3. Post-processing Optimization

Post-treatment optimization plays a pivotal role in electrode fabrication, enhancing electrochemical performance by precisely tailoring chemical composition and surface properties of as-synthesized electrodes.

### 3.3.1. Reduction Treatments

Reduction treatments, such as thermal annealing in  $\text{H}_2$  or  $\text{H}_2/\text{Ar}$  atmospheres, effectively eliminate surface oxides and enhance electrical conductivity [48]. For example,  $\text{MoO}_3/\text{MoSi}_2$  composites transform into metallic-phase  $\text{Mo}_2\text{C}$  when annealed in  $\text{CH}_4/\text{H}_2$ , resulting in a 100-fold increase in conductivity [52]. Likewise,  $\text{H}_2$ -annealed TiN electrodes exhibit 40% lower charge transfer resistance in acidic media due to reduced surface oxygen, significantly improving electrochemical kinetics [48].

### 3.3.2. Surface Modification Techniques

**Table 3.** Comparison of fabrication technologies

Techniques	Key Parameters	Advantages	Limitations	Ref.
Sintering	1400–1600°C, Ar atmosphere	High mechanical strength, scalability	High energy consumption	[45]
Slurry coating + sintering	Slurry solid content: 30–50 wt%	Large-area fabrication	Risk of delamination/pinholes	[52]
Electrospinning	Voltage: 10–20 kV, fiber diameter: 100–500 nm	Ultrahigh specific surface area	Low production efficiency	[52]
3D printing (DIW)	Pore precision: <100 $\mu\text{m}$	Customizable pore structures	High cost of ceramic inks	[52]
Reduction treatment	$\text{H}_2/\text{Ar}$ atmosphere, 500–800°C	Improved conductivity	Risk of structural oxidation	[52]

Surface modification via electrodeposition enables precise control over catalyst nanoparticle size and distribution on ceramic substrates, significantly enhancing catalytic activity. For example, Ni electrodeposition on TiC forms well-defined Ni@TiC heterostructures, where 5–10 nm Ni nanoparticles serve as efficient bifunctional catalysts, demonstrating exceptional HER (60 mV) and OER (138 mV) overpotentials in alkaline media [40]. Crucially, this approach ensures strong metal-ceramic adhesion, preventing catalyst detachment during prolonged operation and maintaining electrode stability.

## 4. Performance Evaluation and Optimization

### 4.1. Key Performance Indicators

The practical utility of electrocatalytic materials hinges on achieving balanced performance across multiple critical parameters, necessitating multidimensional optimization strategies to synergistically enhance structure-activity relationships. A systematic evaluation framework must focus on three key performance metrics: (1) catalytic activity (quantified by overpotential and Tafel slope), (2) operational stability (assessed via long-term durability testing), and (3) mass transfer efficiency (governed by electrode architecture and electrolyte interaction).

#### 4.1.1. Catalytic Activity Metrics and Material Performance

Catalytic activity governs the energy-conversion efficiency of electrocatalytic materials, with overpotential ( $\eta@10 \text{ mA/cm}^2$ ) and Tafel slope serving as the primary descriptors of performance. A low  $\eta$  minimizes thermodynamic overpotential losses, while a small Tafel slope suggests rapid charge-transfer kinetics. However, in proton-coupled reactions, hydrolysis-induced proton generation can introduce kinetic bottlenecks, deteriorating performance [46]. Experimental data reveal significant variations in catalytic performance across different materials. For instance:  $\text{Co}_{0.66}\text{Fe}_{0.33}\text{P}/\text{TiC}_{0.5}\text{N}_{0.5}$  demonstrates outstanding HER activity in alkaline media, achieving an overpotential of 70.4 mV (@10 mA/cm<sup>2</sup>) and a Tafel slope of 40.5 mV/dec, indicative of both high catalytic efficiency and favorable reaction kinetics [53]. In contrast, TiC@MoS<sub>2</sub> exhibits a higher overpotential of 127 mV (@10 mA/cm<sup>2</sup>), highlighting a moderate reduction in activity. Nevertheless, this system underscores the catalytic enhancement effect of carbide supports on sulfide-based electrocatalysts [54]. NCTN-350-2 further showcases exceptional HER performance, with an ultralow overpotential of 66 mV (@10 mA/cm<sup>2</sup>)—significantly lower than bare TiN (483 mV), NCTN precursor (170 mV), and NCCC-350-2 (308 mV), and approaching that of the benchmark Pt electrode (39 mV) (Figure 3a, 3c). This performance enhancement is attributed to the formation of a Co<sub>2</sub>N/TiN heterointerface, which substantially improves charge transfer and catalytic activity. Correspondingly, the Tafel slope of NCTN-350-2 (56 mV/dec) is markedly smaller than those of TiN (145 mV/dec), NCTN precursor (108 mV/dec), and NCCC-350-2 (172 mV/dec), and closely approximates the Pt reference (37 mV/dec) (Figure 3d). These results further confirm its superior reaction kinetics.

The evaluation of OER catalytic performance follows a similar framework to HER, using overpotential and Tafel slope as key metrics. As illustrated in Figure 3b, distinct catalytic behaviors emerge across different samples. The corresponding Tafel plots derived from polarization curves provide further insight into the OER reaction kinetics (Figure 3e). Comparative analysis reveals that optimized samples (e.g., NCTN-350-2) demonstrate superior performance, exhibiting both lower overpotentials and smaller Tafel slopes at 10 mA/cm<sup>2</sup> (Figure 3f). This enhanced catalytic activity suggests more efficient reaction kinetics, which facilitates the generation of oxygen-related species and promotes the overall water-splitting process. Notably, the bifunctional catalyst Ni@TiC achieves an outstanding OER overpotential of 138 mV, demonstrating its potential for practical applications in complete water-splitting systems [55].

Bifunctional catalysts are essential for unifying HER and OER in overall water splitting. The NCTN-250-3||NCTN-350-2 electrolyzer demonstrates spatially decoupled HER/OER activity (Figure 3g), with polarization performance approaching that of RuO<sub>2</sub>||Pt (Figure 3h). This integrated system not only avoids the inefficiencies of mixed-phased catalysts but also reduces overpotentials by optimizing interfacial charge transfer. Crucially, such bifunctional designs lower manufacturing costs by consolidating catalyst materials, presenting a scalable pathway for green hydrogen production.

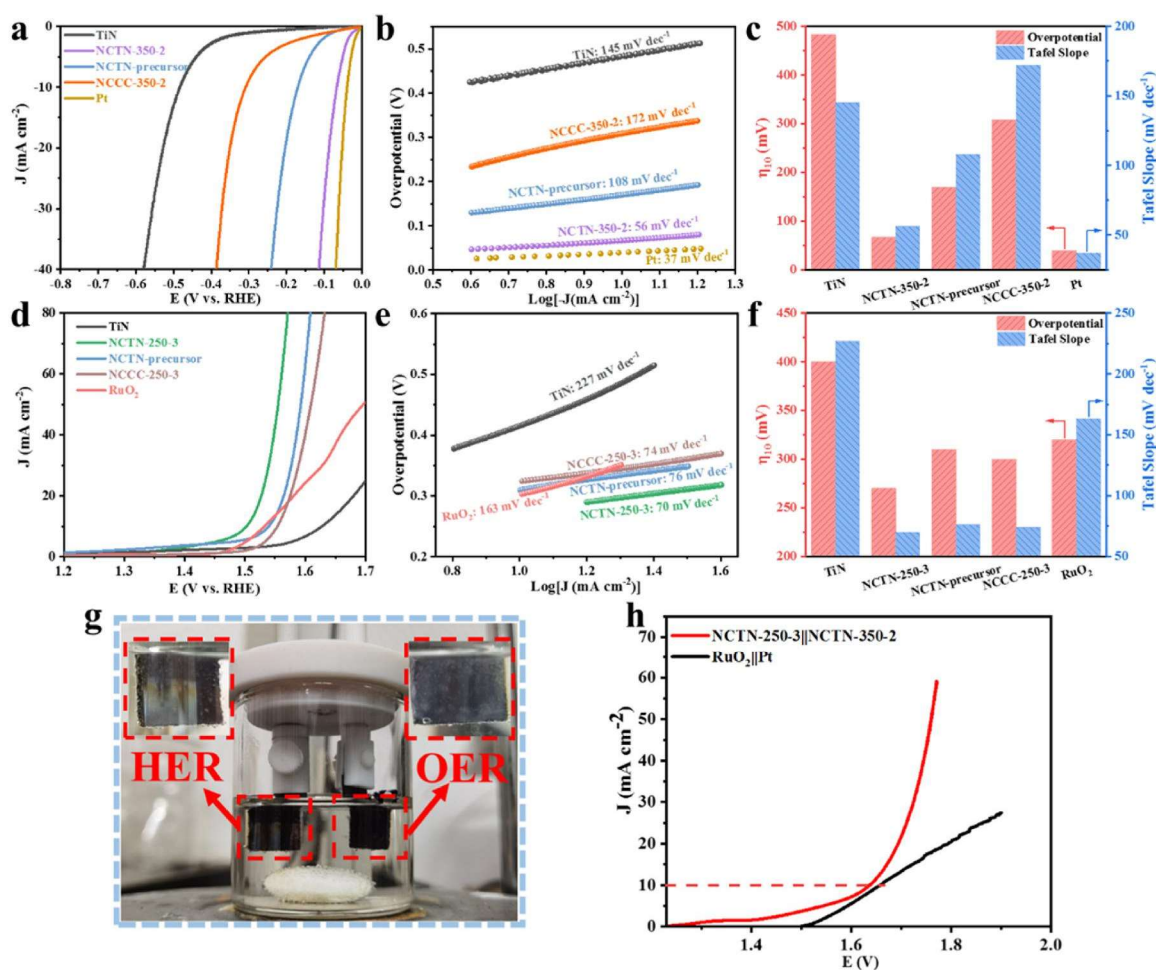


**Figure 3.** (a) HER polarization curves, (b) Tafel plots, (c) overpotentials at 10 mA cm<sup>-2</sup> and Tafel slopes of different samples in 1 M KOH. (d) OER polarization curves, (e) Tafel plots, (f) overpotentials at 10 mA cm<sup>-2</sup> and Tafel slopes of different samples in 1 M KOH. (g) The NCTN-250-3 (anode)||NCTN-350-2 (cathode) two-electrode electrolyzer and (h) its polarization curve for overall water splitting (RuO<sub>2</sub> || Pt was used as reference) [45].

#### 4.1.2. Long-term Stability

To achieve practical viability, electrocatalytic materials must demonstrate exceptional long-term stability, ideally maintaining performance for >1000 hours without significant degradation. Current studies highlight promising durability in various systems: MoO<sub>2</sub>/MoSi<sub>2</sub> exhibits stable operation for 260 hours across a wide current density range (10–1000 mA/cm<sup>2</sup>) [48]. WC-N/W electrodes maintain stability over 220 hours under variable current conditions in acidic media, underscoring the corrosion resistance of carbide/silicide-based materials [36]. Ni@TiC shows no degradation after 50,000 CV cycles, demonstrating the durability-enhancing effect of interfacial synergy [55]. Further evidence of stability is provided by hy-Pd@TaC, which sustains a stable current density of ~50 mA cm<sup>-2</sup> over 21 hours of chronoamperometry (i-t curve). Product analysis reveals a consistent FE(HCOOH) of ~45–50% during testing, with only

a minor decline from 49.8% after 9 hours [41], indicating robust electrode stability. Despite these advances, further improvements are needed to meet the 1000-hour benchmark required for industrial applications.

#### 4.1.3. Mass Transfer Capability

Efficient mass transfer capability is essential for maintaining stable performance under high current densities and is critically dependent on the rational design of material microstructures. TiN and WC electrodes featuring aligned macro-porous channels (50-100  $\mu\text{m}$ ) significantly mitigate gas diffusion limitations, achieving a hydrogen diffusion coefficient of  $8.2 \times 10^{-8} \text{ cm}^2 \cdot \text{s}^{-1}$  and demonstrating a 3-fold enhancement in bubble detachment kinetics compared to conventional electrodes. This structural design enables stable high-current-density operation by facilitating rapid mass transport [36]. The electrochemical active area (ECSA) critically determines the density of available active sites. While quantitative ECSA measurements are not reported, defect engineering strategies-particularly the introduction of oxygen and carbon vacancies-along with compositional tuning can substantially expand the ECSA. For instance, oxygen-deficient  $\text{WO}_{3-x}$  demonstrates enhanced adsorption characteristics that lead to improved catalytic efficiency [40].

#### 4.2. Optimizing Strategy

To overcome the performance limitations of electrocatalytic materials, researchers have adopted a synergistic approach combining composition regulation, interface engineering, and defect engineering, leading to enhanced catalytic activity, stability, and conductivity. Composition regulation serves as a fundamental strategy to improve catalytic performance by fine-tuning the material's electronic structure [36]. For instance, bimetallic doping (e.g.,  $\text{Co}_{0.9}\text{Ni}_{0.1}\text{P}$ ) reduces the hydrogen adsorption energy barrier, significantly boosting the hydrogen evolution reaction (HER) activity [53]. Similarly, Sr-doped perovskite oxides (e.g.,  $\text{LaCoO}_3$ ) enhance the oxygen evolution reaction (OER) by increasing oxygen vacancy concentration, thereby optimizing oxygen species adsorption/desorption kinetics and enabling bifunctional catalysis [40]. Additionally, studies show that the catalytic performance of molybdenum-boron compounds is highly dependent on boron content and structural configuration, highlighting the critical role of electronic state modulation via interelement effects [46].

Constructing heterointerfaces has emerged as a highly effective strategy for enhancing the intrinsic activity of electrocatalytic electrodes [52]. Interface engineering facilitates charge transfer and minimizes interfacial resistance through the strategic design of heterojunctions. For instance, systems such as  $\text{MoO}_2/\text{MoSi}_2$  and  $\text{WC-N/W}$  leverage built-in electric fields to accelerate interfacial charge separation and migration, leading to a 40% increase in HER activity (e.g.,  $\text{MoO}_2/\text{MoSi}_2$ ) [29]. Similarly,  $\text{Co}_{0.9}\text{Ni}_{0.1}\text{P}/\text{TiC}_{0.5}\text{N}_{0.5}$  exhibits an exceptionally low charge transfer resistance ( $R_{\text{ct}} = 0.324 \Omega$ ) [56], further validating the role of heterojunctions in improving charge conduction. Beyond charge transport, heterointerface formation also optimizes the adsorption energy of reaction intermediates via synergistic electronic effects, overcoming the performance limitations of single-component catalysts.

As a pivotal strategy for increasing active site density and improving conductivity, defect engineering enables precise performance modulation through the controlled introduction of defects (e.g., vacancies and dopant atoms) [40]. For instance: Nitrogen-doped WC with engineered carbon vacancies achieves an exceptional conductivity of  $1.4 \times 10^5 \text{ S/m}$  while simultaneously enhancing  $\text{H}^+$  adsorption capacity. Oxygen-deficient oxides (e.g.,  $\text{WO}_{3-x}$  and  $\text{TiO}_{2-x}$ ) utilize oxygen vacancies as active centers, significantly boosting OER/HER bifunctional activity [57]. However, defect concentration and distribution must be carefully optimized-excessive defects can compromise structural stability. Computational-guided design (e.g., DFT

calculations) is therefore essential to tailor defect types and densities for optimal catalytic performance.

In summary, optimizing the performance of electrocatalytic materials requires a balanced synergy among three critical factors: (1) the density of active centers, (2) electron conduction efficiency, and (3) mass transport capability. Moving forward, future research should prioritize the integrated design of multi-strategy approaches (e.g., composition-defect synergy, interface-vacancy coupling) to achieve electrocatalysts that simultaneously meet the practical demands of high activity, long-term stability, and cost-effectiveness.

## 5. Challenges and Limitations

### 5.1. Material Level

The large-scale adoption of electrocatalytic materials continues to face multi-faceted barriers across three critical dimensions: (1) intrinsic material limitations, (2) scalable synthesis challenges, and (3) system-level integration constraints. Addressing these interconnected hurdles requires cross-scale innovation—from atomic-scale active site engineering to macroscopic device optimization—to achieve commercially viable solutions.

At the fundamental materials level, resolving two critical performance trade-offs is essential for advancing electrocatalytic systems. The primary challenge involves optimizing the competing demands of electrical conductivity and catalytic activity in functional materials. Catalytically active materials such as nonstoichiometric tungsten oxide ( $\text{WO}_{3-x}$ ) demonstrate excellent reaction kinetics owing to their abundant oxygen vacancy defects. However, these same materials typically exhibit poor intrinsic conductivity due to: a wide bandgap characteristic of hexavalent tungsten oxides ( $\text{WO}_3$  bandgap  $\sim 2.6$  eV) and limited charge carrier mobility in vacancy-rich structures [58,59]. The pursuit of enhanced conductivity presents a double-edged sword: although conductive additives improve charge transport, they may simultaneously obstruct active sites or modify their electronic properties. This fundamental compromise necessitates nanoscale tailoring of electronic structures to achieve an optimal balance between these competing factors. Recent studies have increasingly emphasized self-supported electrodes due to their ability to facilitate in situ generation of catalytically active phases, thereby improving structural integrity, charge transfer kinetics, and mass transport [60]. Despite these advantages, ceramic-based materials exhibit inherent stability limitations under extreme conditions.  $\text{MoO}_2$ , for instance, suffers from particle detachment in alkaline media due to corrosion-driven interfacial degradation, while WC undergoes surface oxidation in acidic environments, progressively deactivating catalytic sites [48]. Moreover, even protective layers such as  $\text{SiOC}$  are prone to microcrack formation at high temperatures, further exacerbating material degradation. Collectively, these factors impose critical constraints on long-term operational viability [29].

### 5.2. Process Level

Scalability challenges in catalytic material production stem from two key barriers: (1) the trade-off between structural optimization and manufacturability, and (2) process-induced defects. Pore-engineered architectures (e.g., directional channels) enhance mass transport but rely on methods like freeze-drying, where pore size variability ( $\pm 15\%$ ) and cost inefficiencies impede scale-up [29]. Meanwhile, sintering—a critical consolidation step—introduces defects ranging from SiC membrane cracking (thermal stress mismatch) to delamination in tape-cast layers ( $\pm 2\%$  solid content tolerance) [61]. Such processing artifacts not only reduce throughput but also degrade performance via compromised microstructure, demanding near-atomic-level process parameterization for industrial viability.

### 5.3. System Integration

In system integration, compatibility between materials and devices limits performance. A typical issue is poor interfacial contact between electrocatalytic materials and polymer membranes (e.g., PEM). Differences in surface energy and mismatched thermal expansion coefficients lead to high interfacial resistance (reaching  $50 \text{ m}\Omega\cdot\text{cm}^2$  in some systems), significantly increasing energy loss [36]. Compatibility with liquid electrolytes also requires attention: ceramic electrodes may dissolve or corrode in electrolytes, increasing interfacial impedance, while insufficient electrolyte wettability hinders mass transport. Additionally, the incompatibility between rigid ceramic electrodes and flexible devices (e.g., for wearable applications) further restricts use cases, highlighting the need to synergistically design mechanical and functional properties of materials [62].

In summary, addressing these challenges requires interdisciplinary integration of materials chemistry, chemical engineering, and device engineering. A multi-scale regulatory strategy is needed to achieve balanced optimization of "material performance-fabrication cost-system compatibility."

## 6. Future Perspectives

### 6.1. Exploration of Emerging Materials

High-entropy ceramics, leveraging the synergistic effects of multiple elements, are expected to enhance the chemical stability and corrosion resistance of self-supported ceramic electrodes (SSCEs), demonstrating application potential in complex electrolytic environments [53]. Two-dimensional MXenes (e.g.,  $\text{Ti}_3\text{C}_2$ ) possess excellent electrical conductivity. By compounding them with ceramic materials having outstanding stability (such as  $\text{MoSi}_2$ ) to form MXenes-based composite electrodes ( $\text{Ti}_3\text{C}_2/\text{MoSi}_2$ ), the conductivity and stability of the electrodes can be synergistically optimized, providing a new material system for breaking through the performance limitations of SSCEs [29].

### 6.2. Intelligent Manufacturing Technologies

Machine learning is utilized to assist in the component design of electrode materials and the optimization of slurry formulations. Through data-driven approaches, the cost of trial and error is reduced, enabling efficient research and development of material formulations [63]. The development of automated preparation processes, including the use of 3D printing technology to precisely control the pore structure of electrodes for optimizing mass transfer efficiency, and the research and development of continuous phase inversion tape casting methods, will promote the large-scale and low-cost production of SSCEs [29].

### 6.3. Coupled Systems

The coupling of self-supported ceramic electrodes (SSCEs) with photo-electrocatalytic (PEC) systems is expected to realize efficient solar-driven hydrogen production, improving energy conversion and utilization efficiency (Figure 4) [63]. Exploring the application of SSCEs in high-temperature  $\text{CO}_2$  co-electrolysis, while expanding the performance testing of SSCEs in scenarios such as seawater and industrial wastewater electrolysis, will broaden their practical application scope [29]. In addition, in-depth studies on the electron transfer mechanism at the heterojunction interface through in-situ characterization techniques (e.g., in-situ XRD/XPS) will provide theoretical guidance for the design of high-efficiency electrodes in coupled systems, contributing to the performance optimization of coupled systems [29]. The coupling of self-supported ceramic electrodes with photo-electrocatalytic systems has been reported to enhance solar-driven hydrogen production efficiency.

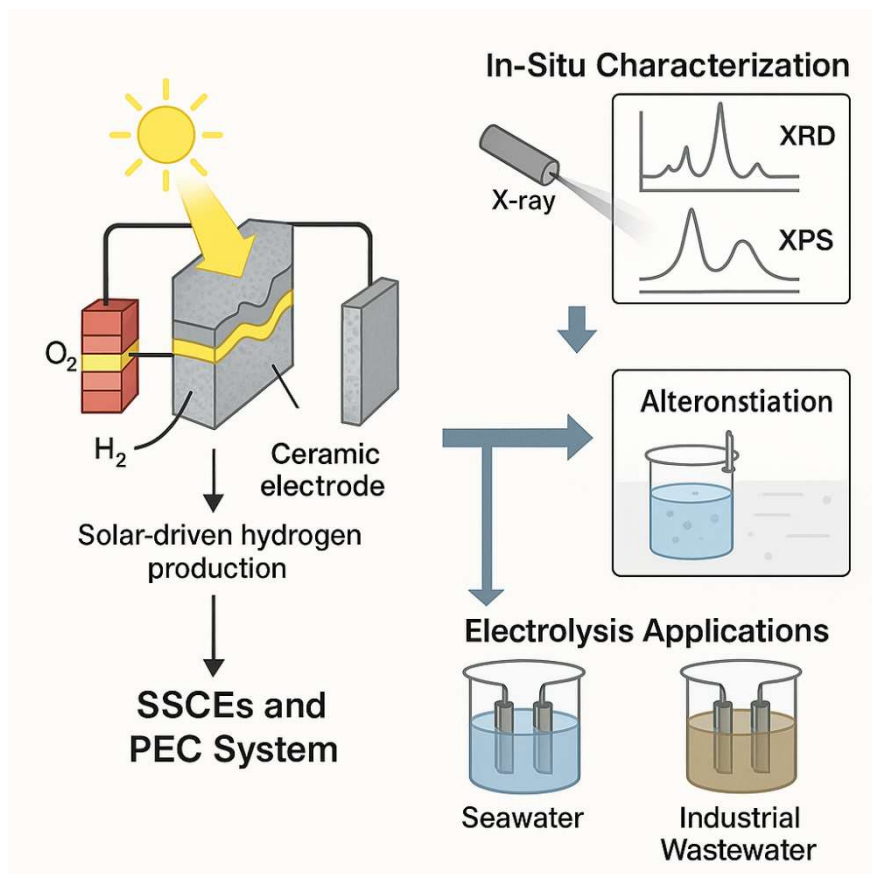


**Figure 4.** The coupling of SSCEs with photo-electrocatalytic (PEC) systems [63].

## 7. Conclusion

### 7.1. Core Advantages and Research Progress

Self-supported ceramic electrodes (SSCEs) demonstrate significant advantages in the field of water electrolysis, integrating high activity (low overpotential), high stability (long lifespan), and high durability (mechanical and chemical stability). Through key technical approaches such as porous structure design, heterojunction construction, and defect regulation, their performance has gradually approached that of noble metal catalysts, providing a highly promising alternative material option for hydrogen production via water electrolysis. However, issues such as insufficient material stability, difficulties in large-scale fabrication, and poor system compatibility remain major bottlenecks hindering their industrialization process.

### 7.2. Importance of Interdisciplinary Collaboration

Promoting the industrial application of SSCEs urgently requires in-depth interdisciplinary integration and collaboration among materials science, electrochemistry, and engineering. The field of materials science can facilitate the development of new materials such as high-entropy ceramics to enhance electrode performance; electrochemical research can provide theoretical support for analyzing electrode reaction mechanisms and optimizing performance; engineering can drive the optimization of preparation processes such as 3D printing and the integration of coupled systems, addressing technical challenges in large-scale production and practical applications. Only through interdisciplinary collaborative innovation can the industrialization of SSCEs be accelerated, enabling them to become a core material pillar for the development of the hydrogen energy economy.

## Acknowledgments

This work was financially supported by the Jiangsu Province's "Double Innovation doctor" project (JSSCBS20221612).

## References

- [1] Z. Ma, T. Wan, D. Zhang, et al. Atomically dispersed Cu catalysts on sulfide-derived defective Ag nanowires for electrochemical CO<sub>2</sub> reduction, *ACS Nano* 17 (2023) 2387–2398.
- [2] a) C. Choi, J. Cai, C. Lee, et al. Huang, Intimate atomic Cu-Ag interfaces for high CO<sub>2</sub>RR selectivity towards CH<sub>4</sub> at low over potential, *Nano Res.* 14 (2021) 3497–3501. b) Feihong Wang. Application of ceramic membrane with straight - pore structure in hydrogen production and water treatment (Doctoral dissertation, University of Science and Technology of China, China 2022). p.1-147.
- [3] Y. Liu, J. Zhang, Y. Li, et al. Manipulating dehydrogenation kinetics through dual-doping Co<sub>3</sub>N electrode enables highly efficient hydrazine oxidation assisting self-powered H<sub>2</sub> production, *Nat. Commun.* 11 (2020) 1853.
- [4] S. Bai, C. Wang, M. Deng, et al. Xiong, Surface polarization matters: enhancing the hydrogen-evolution reaction by shrinking Pt shells in Pt–Pd–graphene stack structures, *Angew. Chem. Int. Ed.* 53 (2014) 12120-12124.
- [5] I. Katsounaros, S. Cherevko, A.R. Zeradjanin, et al. Oxygen electrochemistry as a cornerstone for sustainable energy conversion, *Angew. Chem. Int. Ed.* 53 (2014) 102-121.
- [6] J. Zhang, W. Luo, A. Züttel, Self-supported copper-based gas diffusion electrodes for CO<sub>2</sub> electrochemical reduction, *J. Mater. Chem. A* 7 (2019) 26285-26292.
- [7] W.B. Wu, J.Y. Zhu, Y. Tong, et al. Electronic structural engineering of bimetallic Bi-Cu alloying nanosheet for highly-efficient CO<sub>2</sub> electroreduction and Zn-CO<sub>2</sub> batteries, *Nano Res* 17 (2024) 3684–3692.
- [8] Z.S. Ma, T.Y. Zhang, L.L. Lin, et al. Ni Single-Atom Arrays as Self-Supported Electrocatalysts for CO<sub>2</sub>RR, *Aiche Journal*, 2023.
- [9] B. Xiong, Q. Kang, M. Su, et al. A high-performance self-supported multifunctional NF@Pt electrocatalyst for overall water splitting and rechargeable zinc-air battery, *J. Power Sources* 579 (2023) 233262.
- [10] Z. Yu, K. Mao, Y. Feng, Single-source-precursor synthesis of porous W-containing SiC-based nanocomposites as hydrogen evolution reaction electrocatalysts. *J. Adv. Ceram.* 10 (2021) 1338–1349.
- [11] F. Wang, Z. Xiao, X. Liu, et al. Strategic design of cellulose nanofibers@zeolitic imidazolate frameworks derived mesoporous carbon-supported nanoscale CoFe<sub>2</sub>O<sub>4</sub>/CoFe hybrid composition as trifunctional electrocatalyst for Zn-air battery and self-powered overall water-splitting, *J. Power Sources* 521 (2022) 230925.
- [12] Z. Liu, F. Guo, L. Han, et al. Manganese oxide/iron carbide encapsulated in nitrogen and boron codoped carbon nanowire networks as accelerated alkaline hydrogen evolution and oxygen reduction bifunctional electrocatalysts. *ACS Appl. Mater. Interfaces* 14 (2022) 13280-13294.
- [13] Z. Kou, T. Wang, Z. Pu, et al. Defect-rich MoS<sub>2</sub> ultrathin nanosheets grown on N-doped carbon foam for efficient hydrogen evolution. *Nanoscale Horiz.* 2019, 4,196.
- [14] W. Liu, X. Wang, F. Wang, et al. Boosting CO<sub>2</sub> electroreduction to formate over SnS<sub>2</sub> via phase engineering. *Nat. Commun.* 2021, 12, 6776.
- [15] H. Fan, H. Yu, Y. Zhang, et al. Fe-Doped Ni<sub>3</sub>C Nanodots in N-Doped Carbon Nanosheets for Efficient Hydrogen-Evolution and Oxygen-Evolution Electrocatalysis. *Angew. Chem., Int. Ed.* 2017, 56, 12566.
- [16] Y. Qin, G. Zheng, L. Zhu, et al. Preparation and properties of MoSi<sub>2</sub>-SiC composite coating on Nb-based alloy by pack cementation. *Surf. Coat. Technol.* 2018, 342, 137.
- [17] E. B. Clark, B. Roebuck, The oxidation of MoSi<sub>2</sub> and MoSi<sub>2</sub>-based composites. *Int. J. Refract. Met. Hard Mater.* 1992, 11, 23.

- [18] J. Pirso, S. Letunoviš, M. Viljus, Sliding wear of plasma-sprayed MoSi<sub>2</sub>-based coatings. *Wear* 2004, 257, 257.
- [19] L. Zhong, G. Geng, Y. Wang, et al. Nano-(Ta, Zr)C precipitates at multigrain conjunctions in TaC ceramic with 10 mol% ZrC and 5 mol% Cu as sintering aid. *J. Nanomater.* 2018 (2018) 1634814.
- [20] D. Ni, Y. Cheng, J. Zhang, et al. Advances in ultra-high temperature ceramics, composites, and coatings. *J. Adv. Ceram.* 11 (2022) 1–56.
- [21] F. Winterhalter, V. Medri, A. Ruffini, et al. Corrosion of Si<sub>3</sub>N<sub>4</sub>-MoSi<sub>2</sub> ceramic composite in acid- and basic-aqueous environments: surface modification and properties degradation. *Appl. Surf. Sci.* 2004, 225, 100–115.
- [22] Y. Feng, Z. Yu, J. Schuch, et al. Nowotny phase Mo<sub>3+2x</sub>Si<sub>3</sub>C<sub>0.6</sub> dispersed in a porous SiC/C matrix: A novel catalyst for hydrogen evolution reaction. *J. Am. Ceram. Soc.* 2019, 103, 508–519.
- [23] Y. Cao, Road map and Direction Toward High-Performance MoS<sub>2</sub> Hydrogen Evolution Catalysts. *ACS Nano* 2021, 15 (7), 11014–11039.
- [24] Y. Sun, F. Alimohammadi, D Zhang, et al. Enabling Colloidal Synthesis of Edge-Oriented MoS<sub>2</sub> with Expanded Interlayer Spacing for Enhanced HER Catalysis. *Nano Lett.* 2017, 17 (3), 1963–1969.
- [25] L. Zhang, Z. Hu, J. Huang, et al. Experimental and DFT Studies of Flower-like Ni-Doped Mo<sub>2</sub>C on Carbon Fiber Paper: A Highly Efficient and Robust HER Electro-catalyst Modulated by Ni(NO<sub>3</sub>)<sub>2</sub> Concentration. *J. Adv. Ceram.* 2022, 11 (8), 1294–1306.
- [26] R. Mir, O. Pandey, Influence of Graphitic/Amorphous Coated Carbon on HER Activity of Low Temperature Synthesized β-Mo<sub>2</sub>C@C Nanocomposites. *Chem. Eng. J.* 2018, 348, 1037–1048.
- [27] H. Yan, Y. Xie, Y. Jiao, et al. Holey Reduced Graphene Oxide Coupled with an Mo<sub>2</sub>N-Mo<sub>2</sub>C Heterojunction for Efficient Hydrogen Evolution. *Adv. Mater.* 2018, 30 (2).
- [28] B. Zhang, H. Xu, Q. Chen, et al. ZIF-67 Derived Mo<sub>2</sub>N/Mo<sub>2</sub>C Heterostructure as High-Efficiency Electrocatalyst for Hydrogen Evolution Reaction. *J. Alloys Compd.* 2022, 922, 166216.
- [29] Nianwang Ke. Application of Mo-based ceramic membrane in hydrogen production and hydrogen storage [D]. University of Science and Technology of China, 2023.
- [30] Y. Jin, H. Wang, J. Li, et al. Porous MoO<sub>2</sub> Nanosheets as Non-noble Bifunctional Electro catalysts for Overall Water Splitting. *Adv. Mater.* 2016, 28, 3785–3790.
- [31] X. Xie, L. Lin, R.-Y. Liu, et al. The synergistic effect of metallic molybdenum dioxide nanoparticle decorated graphene as an active electrocatalyst for an enhanced hydrogen evolution reaction. *J. Mater. Chem. A* 2015, 3, 8055–8061
- [32] Yutong Wu. Preparation of Self-supported Transition Metal Catalytic Electrode and Mechanism Research on Water Electrolysis (Master's dissertation, University of Science and Technology of China, China 2022). p.1-66.
- [33] Kai Lv. Preparation of Ceramic Electrode Based Titanium Nitride for Water Electrolysis (Master's dissertation, University of Science and Technology of China, China 2021). p.1-89.
- [34] a) Y. Shi, D. Zheng, X. Zhang, K. Lv, F. Wang, B. Dong, S. Wang, C. Yang, J. Li, F. Yang, L. Y. Hao, L. Yin, X. Xu, Y. Xian, S. Agathopoulos, *Chem. Mater.* 2021, 33, 6217; b) K. Lv, D. Zheng, Y. Shi, X. Zhang, F. Wang, J. Li, S. Wang, B. Dong, L. Y. Hao, L. Yin, X. Xu, Y. Xian, S. Agathopoulos, *ACS Appl. Energy Mater.* 2021, 4, 6730.
- [35] J. Su, Y. Yang, G. Xia, J. Chen, P. Jiang, Q. Chen, *Nat. Commun.* 2017, 8, 14969.
- [36] F. Wang, Y. Wu, B. Dong, et al. Robust Porous WC-Based Self-Supported Ceramic Electrodes for High Current Density Hydrogen Evolution Reaction. *Advanced Science.* 2022, 9, 2106029.
- [37] F. Tan, J. Zhang, Y. Zhang, et al. Influence of Pore - forming Process and SiC Nanowires on the Structure and Properties of SiOC Porous Ceramics. *Chinese Journal of Rare Metals*, 2023, 47(8): 1178 - 1185.
- [38] Youcheng Wu. Preparation and Properties of 3D self-supporting structure electrocatalytic hydrogen production materials[D]. Hunan Agricultural University, 2021.

- [39] Yangyang Shi. Study on Preparation of Titanium Carbide-based Ceramic Electrode and Application of Water Electrolysis (Master's dissertation, University of Science and Technology of China, China 2021). p.1-57.
- [40] C. Tan, H. Huang, F. Wang, et al. Porous TiN-based ceramic electrode with N-modified Co-based Nanorods/TiN heterointerfaces for efficient overall water splitting. *Journal of Power Sources*. 2024, 610, 234722.
- [41] Q. Zhong, A. Huang, W. Tang, et al. Hydrophobic self - supported nano - Pd - embedded TaC ceramic membrane electrode for electrochemical reduction of CO<sub>2</sub> to formate. *Ceramics International*. 2025, 51, 23133-23139.
- [42] N. Ke, H. Huang, F. Wang, et al. Self-supported MoO<sub>2</sub>/MoSi<sub>2</sub> ceramic electrode for high current density hydrogen evolution reaction. *ACS Sustain. Chem. Eng.* 11 (2023) 3769-3779.
- [43] Y. Shi, D. Zheng, X. Zhang, et al. Self-supported ceramic electrode of 1T-2H MoS<sub>2</sub> grown on the TiC membrane for hydrogen production. *Chem. Mater.* 33 (2021) 6217-6226.
- [44] Tao. S, Y.D. Xu, J.Q. Gu, et al. Preparation of high-efficiency ceramic planar membrane and its application for water desalination. *J Adv Ceram* 2018, 7: 117-123.
- [45] F.H. Wang, B.B. Dong, N.W. Ke, et al. Superhydrophobic β-sialon-mullite ceramic membranes with high performance in water treatment. *Ceram Int* 2021, 47: 8375-8381.
- [46] K. Lv, D.W. Zheng, Y.Y. Shi, et al. Highly efficient and robust MoS<sub>2</sub> nanoflake-modified-TiN-ceramic-membrane electrode for electrocatalytic hydrogen evolution reaction. *ACS Appl Energy Mater* 2021, 4: 6730-6739.
- [47] Y.Y. Shi, D.W. Zheng, X. Zhang, et al. Self-supported ceramic electrode of 1T-2H MoS<sub>2</sub> grown on the TiC membrane for hydrogen production. *Chem Mater* 2021, 33: 6217-6226.
- [48] N. Ke, H. Huang, F. Wang, et al. Self-Supported MoO<sub>2</sub>/MoSi<sub>2</sub> Ceramic Electrode for High Current Density Hydrogen Evolution Reaction. *ACS Sustainable Chemistry & Engineering*, 2023, 11, 3769-3779.
- [49] Jonathan T Davis, Buddhinie S Jayathilake, Swetha Chandrasekaran, et al. 3D printed optimized electrodes for electrochemical flow reactors. *Sci Rep*, 2024, 14(1):22662.
- [50] L. Chen, R. Lin, M.g Dong, et al. Optimizing the Mass-Transfer Efficiency of a Microporous Layer for High-Performance Proton Exchange Membrane Fuel Cells. *ACS Publications*, 2021.
- [51] K. Yang, S. Zhong, H. Yue, et al. Application of pulsed chemical vapor deposition on the SiO<sub>2</sub>-coated TiO<sub>2</sub> production within a rotary reactor at room temperature. *Chinese Journal of Chemical Engineering*, 2022, 45 (05).
- [52] S. Huang, A. Huang, H. Huang, et al. Self - Supported α-MoB/β-MoB<sub>2</sub> Ceramic Electrodes for Efficient High - Current - Density Hydrogen Evolution in Acidic, Neutral, and Alkaline pH-Values. *ACS Applied Materials & Interfaces*, 2025, 17, 7739 - 7749.
- [53] H. Shao, Y. Wu, X. Xu, et al. Electrocatalytic Self-Supported-Electrode Based on Co<sub>x</sub>Ni<sub>1-x</sub>P/TiC<sub>0.5</sub>N<sub>0.5</sub> for Enhancing pH - Universal Hydrogen Evolution Electrocatalysis. *Adv Sustain Syst*, 2022.
- [54] Y. Shi, D. Zheng, X. Zhang, et al. Self-Supported Ceramic Electrode of 1T-2H MoS<sub>2</sub> Grown on the TiC Membrane for Hydrogen Production. *Chem Mater*, 2021, 33, 6217 - 6226.
- [55] Y. Shi, F. Yang, L. Tao. Ni-Activated and Ni-P-Activated Porous Titanium Carbide Ceramic Electrodes as Efficient Electrocatalysts for Overall Water Splitting. *ACS Appl Mater Interfaces*, 2023, 15, 28055 - 28063.
- [56] Shao Haojie. Preparation of Transition Metal Phosphide/Titanium Carbonitride Self - supported Electrode and Its Application in Water Splitting [D]. University of Science and Technology of China, 2022.
- [57] F. WANG, B. DONG, J. WANG, et al. Self-supported porous heterostructure WC/WO<sub>3-x</sub> ceramic electrode for hydrogen evolution reaction in acidic and alkaline media. *Journal of Advanced Ceramics*, 2022, 11(6): 1208 - 1223.
- [58] A. Huang, H. Huang, F. Wang, et al. Mo<sub>2</sub>C - Based Ceramic Electrode with High Stability and Catalytic Activity for Hydrogen Evolution Reaction at High Current Density. *Small*, 2023.

- [59] Liu, Y, Shrestha, S, Mustain, WE. Synthesis of nanosize tungsten oxide and its evaluation as an electrocatalyst support for oxygen reduction in acid media. *ACS Catal* 2012, 2: 456–463.
- [60] MR Thalji, GAM Ali, H Algarni, et al. Al<sup>3+</sup> ion intercalation pseudocapacitance study of W<sub>18</sub>O<sub>49</sub> nanostructure. *J Power Sources* 2019, 438: 227028.
- [61] Feihong Wang. Application of ceramic membrane with straight - pore structure in hydrogen production and water treatment [D]. University of Science and Technology of China, 2022.
- [62] Weiguo Pu. Preparation and properties of flexible electrochromic devices based on PMMA gel electrolyte [D]. Lanzhou Jiaotong University, 2023.
- [63] Z. Zhu, Z. Liu, Q. Wang, et al. Molten Salt One-Pot Electrosynthesis of a Ni-MoC-Mo<sub>2</sub>C/Mo Self-Supported Electrode for Efficient pH-Universal Hydrogen Evolution. *ACS Appl Energy Mater*, 2023, 6, 12084 - 12094.